


 Cite this: *Phys. Chem. Chem. Phys.*, 2023, 25, 8331

 Received 5th December 2022,  
 Accepted 24th February 2023

DOI: 10.1039/d2cp05678j

rsc.li/pccp

# Effect of stacking interactions on charge transfer states in photoswitches interacting with ion channels†

 Vito F. Palmisano,<sup>ab</sup> Shirin Faraji<sup>id</sup>\*<sup>b</sup> and Juan J. Nogueira<sup>id</sup>\*<sup>ac</sup>

The activity of ion channels can be reversibly photo-controlled via the binding of molecular photoswitches, often based on an azobenzene scaffold. Those azobenzene derivatives interact with aromatic residues of the protein via stacking interactions. In the present work, the effect of face-to-face and t-shaped stacking interactions on the excited state electronic structure of azobenzene and *p*-diaminoazobenzene integrated into the Na<sub>v</sub>1.4 channel is computationally investigated. The formation of a charge transfer state, caused by electron transfer from the protein to the photoswitches, is observed. This state is strongly red shifted when the interaction takes place in a face-to-face orientation and electron donating groups are present on the aromatic ring of the amino acids. The low-energy charge transfer state can interfere with the photoisomerization process after excitation to the bright state by leading to the formation of radical species.

Photopharmacology is establishing a new paradigm to overcome the problem of poor drug selectivity, which is responsible for the discard of most pharmaceuticals in clinical research.<sup>1</sup> The use of chromophoric species as drugs would make it possible to reversibly control in space and time their biological function upon the application of light. This strategy gives the opportunity to create highly selective drugs able to be active at the receptor and inactive before and after reaching its biological target, decreasing its toxicity and side effects.<sup>2</sup> Due to its versatile organic synthesis and photophysics, azobenzene (AZ) is currently the most engaged backbone for developing photoswitchable compounds.<sup>3</sup> AZ is mainly at the trans configuration in the dark (99.9%) and its absorption spectrum presents two well-separated bands in the UV-vis region at 320 (3.87 eV) and

450 (2.75 eV) nm.<sup>4–6</sup> In addition, the quantum yield of photoisomerization is around 0.25 when excited to S<sub>1</sub>(n → π\*) and 0.11 when excited to S<sub>2</sub>(π → π\*).<sup>7,8</sup>

In AZ, chemical modifications at the phenyl rings can induce drastic changes in its excited state electronic structure, improving the photophysics of those compounds.<sup>9</sup> In receptor pharmacology, ion channels were the first targets of photo-control, allowing the remote regulation of neural firing with a synthetic photoswitch.<sup>10</sup> A wide variety of photoswitchable AZ-based compounds have been developed during the last two decades.<sup>11–16</sup> However, no mechanistic studies have been addressed on the effect that the protein environment can play on the absorption spectra and photophysics of the photoswitches, although it is well-known that the environment can strongly modify the electronic structure of chromophores.<sup>17–20</sup> In particular, aromatic stacking has long been recognized as one of the key constituents of ligand–protein interfaces.<sup>21</sup> To this end, we have investigated the effect of different aromatic protein residues on the absorption spectrum and density of states of AZ and *p*-diaminoazobenzene (*p*AZ) embedded in the human brain Na<sub>v</sub>1.4 channel. For comparison, the effect of two different solvents, namely water and hexane, was also investigated. Our analysis shows that the electronic structure of the unsubstituted AZ drastically changes upon interactions with F797 by leading to the appearance of a low-lying charge transfer state (CT) which might interfere with the photoisomerization process.

The absorption spectrum and density of states of AZ and *p*AZ were computed in water, hexane and the human Na<sub>v</sub>1.4 channel (see Fig. 1a) by means of quantum mechanics/molecular mechanics (QM/MM) calculations on top of an ensemble of snapshots taken from classical molecular dynamics (MD). For the calculations of the photoswitches inside the channel, the most stable binding pocket was identified in previous MD simulations.<sup>16</sup> The QM region is formed by the photoswitches and is described at time-dependent density-functional theory (TD-DFT) with the ωB97X-D functional<sup>22</sup> and cc-pVDZ basis set,<sup>23</sup> while the classical region comprises the protein, lipid bilayer, and

<sup>a</sup> Department of Chemistry, Universidad Autónoma de Madrid, 28049, Madrid, Spain. E-mail: juan.nogueira@uam.es

<sup>b</sup> Theoretical Chemistry Group, Zernike Institute for Advanced Materials, University of Groningen, Groningen, The Netherlands. E-mail: s.s.faraji@rug.nl

<sup>c</sup> Institute for Advanced Research in Chemistry (IAChem), Universidad Autónoma de Madrid, Madrid 28049, Spain

† Electronic supplementary information (ESI) available. See DOI: <https://doi.org/10.1039/d2cp05678j>



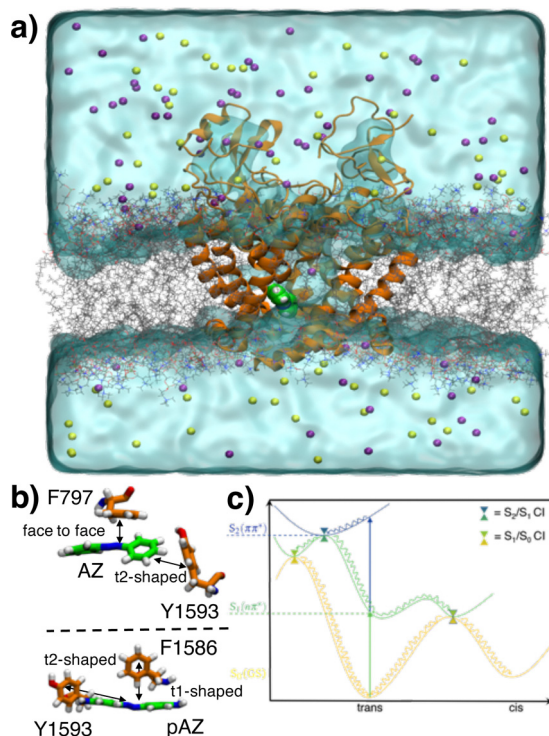


**Fig. 1** (a) Representation of the photoswitch (green) interacting with the Nav1.4 channel (orange) integrated into a membrane (dark gray). Water is represented by the cyan surface and the Na<sup>+</sup> and Cl<sup>-</sup> ions by the yellow and violet beads. (b) Aromatic residues interacting with AZ and pAZ along the MD simulation. Color code: C atoms of the photoswitches in green, C atoms of the protein residues in orange, N atoms in blue, H atoms in white, and O atoms in red. (c) Schematic representation of the deactivation pathways of AZ after excitation to S<sub>1</sub>(nπ\*) and S<sub>2</sub>(ππ\*).

solvents and is described by appropriate force fields. In the case of the systems formed by AZ and pAZ integrated into the channel, a second set of calculations were performed to include the closest aromatic protein residues inside the QM region (see Fig. 1b) and, thus, investigate the appearance of intermolecular CT states. The MoBioTools package was used to extract geometries, split the system in the QM and MM region and prepare the inputs for the QM/MM calculations.<sup>24</sup> The characterization of the nπ\*, ππ\* and CT states was performed with the TheoDOR software, analyzing the transition density matrix.<sup>25</sup> Finally, to rationalize the results found for the photoswitches/protein complexes, the electronically excited states of AZ and pAZ interacting with phenylalanine and tyrosine in a vacuum were computed by ωB97X-D/cc-pVDZ. More computational details can be found in the ESI.†

We start the discussion by analyzing the absorption spectra and density of states of AZ and pAZ (see Fig. 2). In these calculations only the photoswitch is included in the QM region, while the entire environment is described classically. Therefore, this scheme is only able to describe the polarization of the chromophore by the presence of the environment, potentially inducing energy shifts on the different states, but not an active role of the environment on the electronic excitations, where charge transfer events between the chromophore and the environment molecules could occur. This last effect will be

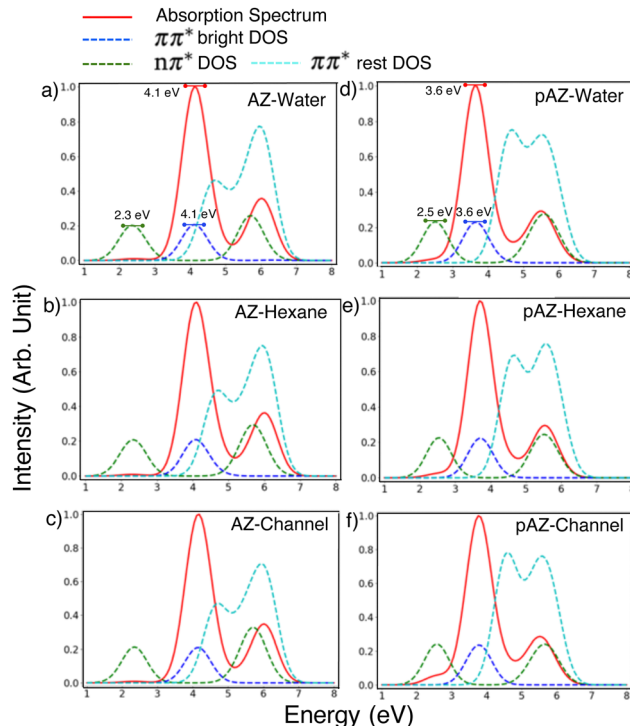


**Fig. 2** Absorption spectra and density of states of AZ (a–c) and pAZ (d–f) interacting with water, hexane and the ion channel. The red lines represent the absorption spectra with normalized values for the oscillator strength. The blue, cyan and green dashed lines represent the density of states of the bright ππ\* state, the other ππ\* states, and the nπ\* states, respectively. The QM layer in the QM/MM scheme only includes the photoswitch.

analyzed later in this work. An important property which affects the photoisomerization yield of the chromophores is the energy gap between the S<sub>1</sub>(nπ\*) and S<sub>2</sub>(ππ\*) states.<sup>9</sup> A recent computational study showed that a hot S<sub>1</sub>(nπ\*) state, reached after internal conversion from the bright state, decays to the ground state through an energetically high lying conical intersection seam, not accessible upon direct excitation to the S<sub>1</sub>(nπ\*) state, as shown in Fig. 1c. This hot decay channel was argued to be nonreactive, explaining the lower isomerization quantum yield after S<sub>2</sub>(ππ\*) excitation in comparison to the S<sub>1</sub>(nπ\*) excitation.<sup>26</sup> The electron donor *p*-diamino substituents induce a decrease in the gap between the S<sub>1</sub>(nπ\*) and S<sub>2</sub>(ππ\*) states. The lower energy separation between these two states leads to a drop of the internal conversion to the hot nonreactive state and, therefore, increases the quantum yield of photoisomerization upon S<sub>2</sub>(ππ\*) excitation.<sup>27</sup> Experimentally, the energy gap at the Franck–Condon region between the S<sub>2</sub>(ππ\*) and S<sub>1</sub>(nπ\*) states was found to be 1.17 eV for AZ, while for pAZ only one absorption band is observed at 2.96 eV due to a higher overlap between the two states.<sup>27</sup> Previous theoretical calculations at the TD-DFT level of AZ and pAZ in a vacuum have predicted an energy gap of 1.22 eV and 0.55 eV, respectively, between S<sub>2</sub>(ππ\*) and S<sub>1</sub>(nπ\*).<sup>28</sup> As shown in Fig. 2a and d, the energy gap predicted by our calculations in water is 1.8 and 1.1 eV for AZ and pAZ, respectively, in qualitative agreement with previous theoretical and experimental trends. However, an accurate quantitative



description of the experimental behaviour is not achieved because of the need of using a range-separated functional to describe CT states between the protein and the photoswitches. The difficulty of describing with the same accuracy both valence and CT states is well known and has been intensively investigated in the last few years.<sup>29,30</sup> In addition, Fig. 2 also shows that the polarizable effect of the different environments (water, hexane and ion channel) on the electronic structure of the chromophores is virtually the same since no important energy shifts on the absorption spectrum and density of states are observed when moving among the different environments.

In the following, the active role of the environment on the electronic excitation is investigated. Specifically, electron transfer processes between the chromophore and the protein residues give rise to the formation of CT states, which could participate in the photophysics of the chromophore and compete with the photoisomerization pathway. In addition, the appearance of intermolecular CT states yields radical species, which are very prone to react and could induce damage in the protein. Therefore, an ideal photoswitch aimed at controlling the activity of voltage-gated ion channels should not participate in CT events with the protein. The MD simulations of AZ and *p*AZ in the Na<sub>v</sub>1.4 channel have revealed important interactions with phenylalanine and tyrosine residues. As shown in Fig. 1b, AZ interacts with F797 in a face-to-face orientation, where the aromatic ring of F797 is parallel to the azo group of AZ, and with Y1593 in a t2-shaped orientation, where the hydrogen atoms of AZ point towards the aromatic ring of Y1593. In the case of *p*AZ, two interactions in t-shaped orientation were found. In the first one, the photoswitch interacts with Y1593 in a t2-shaped orientation, while in the second one *p*AZ interacts with F1586 in a t1-shaped orientation, where the hydrogen atoms of the aromatic ring of F1586 point towards one of the phenyl rings of *p*AZ. The predominance of t-shaped orientations found in our simulations is in agreement with recent experimental datasets of ligand–protein  $\pi\pi$  stacking interactions.<sup>31</sup>

In order to investigate the role of these aromatic residues on the electronically excited states of the photoswitches, four different sets of QM/MM calculations were performed. These calculations differ in the residues included in the QM region: AZ and F797, AZ and Y1593, *p*AZ and Y1593, and *p*AZ and F1586. In this way, electron transfer events between the photoswitches and the phenylalanine and tyrosine residues within the QM region can be modeled. The computed absorption spectra and density of states are displayed in Fig. 3a–d. In all the cases, a CT state characterized by electron transfer from a  $\pi$  orbital of the amino acid to a  $\pi^*$  orbital of the photoswitch is found in the energy range of 5–6 eV, *i.e.*, located more than 1 eV higher in energy than the maximum of the absorption band. However, in the case of AZ, the tail of the CT band extends along the low-energy region up to 4 eV, which is the energy value of the absorption maximum. This means that after excitation to the bright state, the CT state is energetically accessible and could be populated along the dynamics by internal conversion. Interestingly, the CT state for *p*AZ is blue

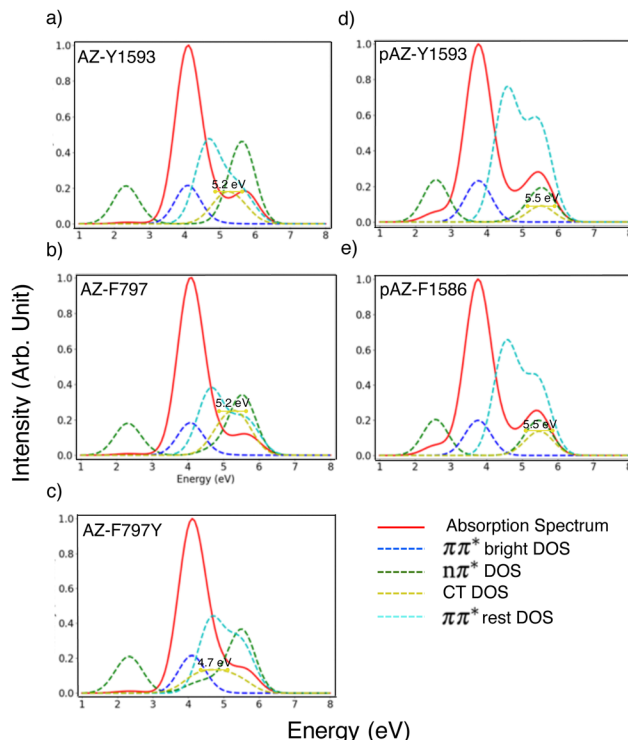


Fig. 3 Absorption spectra and density of states of AZ (a–c) and *p*AZ (d and e) interacting with the ion channel. The red lines represent the absorption spectra with normalized values for the oscillator strength. The blue, cyan, green and yellow dashed lines represent the density of states of the bright  $\pi\pi^*$  state, the other  $\pi\pi^*$  states, the  $\pi\pi^*$  states and the CT states, respectively. The QM layer in the QM/MM scheme includes the photoswitch and the protein residue specified in the legend of each panel.

shifted by 0.3 eV with respect to the CT band of AZ and, therefore, it is difficult to populate after excitation to the bright state.

The blue shift of the CT band of *p*AZ observed in our complex models, which include conformational sampling and the biological environment, can be rationalized based on static electronically excited state calculations for simplified models. These static models do not describe sampling and the environment. Specifically, the geometries of AZ/phenylalanine, AZ/tyrosine, *p*AZ/phenylalanine, and *p*AZ/tyrosine complexes were optimized at the ground state in a vacuum for the face-to-face, t1-shaped and t2-shaped orientations at the DFT level, using  $\omega$ B97X-D/cc-pvdz as the functional and basis set. The t2-shaped minima for *p*AZ were not found, and for all the other systems the excited state energies were computed with TD-DFT and are shown in Fig. 4a. The first conclusion that can be extracted is that the CT state is higher in energy than the bright  $\pi\pi^*$  state for all the complexes but AZ/tyrosine in the face-to-face orientation. In addition, the face-to-face orientations for the AZ/phenylalanine and *p*AZ/tyrosine complexes present a small CT/ $\pi\pi^*$  energy gap in comparison with all the other situations due to the red shift of the CT state. Therefore, the face-to-face orientation favors the energy lowering of the CT state, a fact which is not surprising since this orientation should lead to a



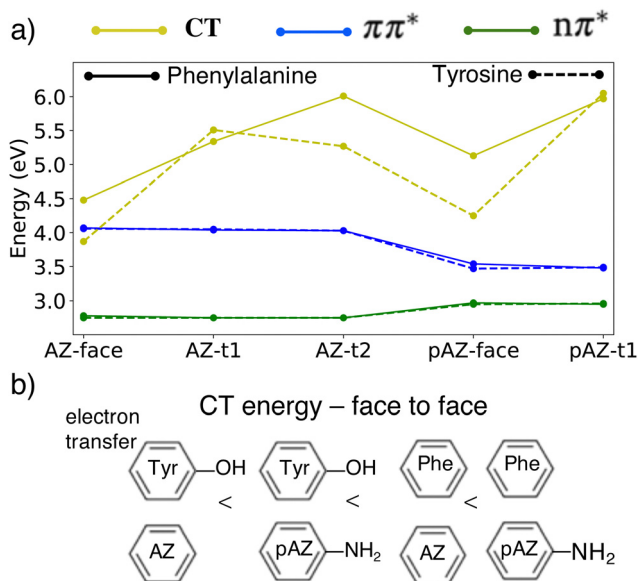


Fig. 4 (a) Excitation energies in a vacuum for AZ and pAZ interacting with phenylalanine and tyrosine in the face-to-face, t1-shaped and t2-shaped conformations. (b) Schematic representation of the energy trend followed by the face-to-face interactions between phenylalanine (Phe) and tyrosine (Tyr) with the photoswitches.

larger orbital overlap between the photoswitches and the amino acids than the t-shaped orientations. These results are also in agreement with theoretical results obtained for the un-, mono- and di-substituted benzene dimer.<sup>32,33</sup> A more interesting trend can be observed when comparing the excited state energies of the photoswitch/phenylalanine and photoswitch/tyrosine complexes. As can be seen, the CT/ $\pi\pi^*$  energy gap is lower when the photoswitch is interacting with tyrosine due to a red shift of the CT state. This can be qualitatively explained by attending to the nature of the CT transition. The CT state is characterized by an electron transfer from a  $\pi$  orbital of the amino acid to a  $\pi^*$  orbital of the photoswitch. Therefore, the residue-to-chromophore electron transfer is favored when the aromatic ring of the protein residue is richer in electrons, as it is the case of tyrosine due to the presence of the electron donating hydroxy group on the phenyl ring, which is absent in phenylalanine.<sup>32</sup> On the contrary, the residue-to-chromophore electron transfer is energetically unfavorable when the aromatic system of the chromophore, which receives the electron, is already rich in electrons, as it is the case in pAZ due to the presence of the electron donating amino substituents. And this is exactly what is observed in Fig. 4a. The energy of the CT states for a given orientation and amino acid is always lower for AZ than for pAZ, for example, AZ/phenylalanine (4.4 eV) against pAZ/phenylalanine (5.1 eV) for the face-to-face orientation.

To corroborate whether the previous conclusions from the vacuum models can be extrapolated to the more realistic model where the ion channel is present, additional QM/MM calculations were performed. We took the last snapshot of the simulation of AZ interacting with the Na<sub>v</sub>1.4 channel, where AZ interacts with F797 in a face-to-face way, and performed the

F797Y mutation in order to have AZ interacting with tyrosine in the face-to-face orientation. An additional MD simulation was evolved on top of which the absorption spectrum and density of states were computed by QM/MM. The resulting bands are displayed in Fig. 3c, showing that the CT band is strongly red-shifted with respect to that of the non-mutated system (Fig. 3b), leading to an overlap with the absorbing band. Therefore, the face-to-face orientation between electron deficient azobenzene photoswitches (either unsubstituted or substituted with electron withdrawing groups) interacting with aromatic residues that are rich in electrons (tyrosine and likely tryptophan) gives rise to low-energy CT states, which can be populated after light excitation.

In conclusion, when the environment is entirely described by a force field, the electronic structure of the photoswitches barely changes when moving across solvents of different polarity and the membrane protein. However, when the aromatic residues of the Na<sub>v</sub>1.4 channel closely interacting with the photoswitches (phenylalanine and tyrosine) are described quantum mechanically, it is found that these residues actively participate in the electronic excitation of both AZ and pAZ. This shows that a quantum mechanical description of some protein residues is required to model the photophysics of the system. Specifically, electron transfer from the protein residues to the photoswitches leads to the formation of a CT state. This state lies low in energy in the face-to-face orientation, especially for the AZ/tyrosine complex, energetically accessible after excitation to the bright state, and could be potentially involved in the deactivation pathway of the photoswitch, decreasing the photoisomerization yield. However, further theoretical work aimed at investigating the excited-state dynamics is needed to corroborate the importance of the CT states. Therefore, a rational design of new photoswitches aimed at controlling the ion channel activity should also take into account the stacking interactions with neighbouring amino acids, and avoid the appearance of the CT state by aromatic substitutions at the AZ rings.

## Conflicts of interest

There are no conflicts to declare.

## References

- 1 K. Hull, J. Morstein and D. Trauner, *Chem. Rev.*, 2018, **118**, 10710–10747.
- 2 W. A. Velema, W. Szymanski and B. L. Feringa, *J. Am. Chem. Soc.*, 2014, **136**, 2178–2191.
- 3 A. A. Beharry and G. A. Woolley, *Chem. Rev.*, 2011, **40**, 4422–4437.
- 4 G. S. Hartley, *Nature*, 1937, **140**, 281.
- 5 A. Mostad and C. Romming, *Acta Chem. Scand.*, 1971, **25**, 3561.
- 6 C. J. Brown, *Acta Crystallogr.*, 1966, **21**, 146–152.
- 7 P. Bortolus and S. Monti, *J. Phys. Chem.*, 1979, **83**, 648–652.



- 8 N. Siampiringue, G. Guyot, S. Monti and P. Bortolus, *J. Photochem.*, 1987, **37**, 185–188.
- 9 H. D. Bandara and S. C. Burdette, *Chem. Soc. Rev.*, 2012, **41**, 1809–1825.
- 10 M. Banghart, K. Borges, E. Isacoff, D. Trauner and R. H. Kramer, *Nat. Neurosci.*, 2004, **7**, 1381–1386.
- 11 A. Mourot, M. A. Kienzler, M. R. Banghart, T. Fehrentz, F. M. Huber, M. Stein, R. H. Kramer and D. Trauner, *ACS Chem. Neurosci.*, 2011, **2**, 536–543.
- 12 A. Mourot, T. Fehrentz, Y. Le Feuvre, C. M. Smith, C. Herold, D. Dalkara, F. Nagy, D. Trauner and R. H. Kramer, *Nat. Methods*, 2012, **9**, 396–402.
- 13 A. Mourot, I. Tochitsky and R. H. Kramer, *Front. Mol. Neurosci.*, 2013, **6**, 5.
- 14 A. Polosukhina, J. Litt, I. Tochitsky, J. Nemargut, Y. Sychev, I. De Kouchkovsky, T. Huang, K. Borges, D. Trauner and R. N. Van Gelder, *Neuron*, 2012, **75**, 271–282.
- 15 I. Tochitsky, A. Polosukhina, V. E. Degtyar, N. Gallerani, C. M. Smith, A. Friedman, R. N. Van Gelder, D. Trauner, D. Kaufer and R. H. Kramer, *Neuron*, 2014, **81**, 800–813.
- 16 V. F. Palmisano, C. Gómez-Rodellar, H. Pollak, G. Cárdenas, B. Corry, S. Faraji and J. J. Nogueira, *Phys. Chem. Chem. Phys.*, 2021, **23**, 3552–3564.
- 17 J. J. Nogueira, M. Oppel and L. González, *Angew. Chem., Int. Ed.*, 2015, **54**, 4375–4378.
- 18 J. J. Nogueira, S. Roßbach, C. Ochsenfeld and L. González, *J. Chem. Theory Comput.*, 2018, **14**, 4298–4308.
- 19 J. J. Nogueira, M. Meixner, M. Bittermann and L. González, *ChemPhotoChem*, 2017, **1**, 178–182.
- 20 M. De Vetta, M. F. S. J. Menger, J. J. Nogueira and L. González, *J. Phys. Chem. B*, 2018, **122**, 2975–2984.
- 21 E. A. Meyer, R. K. Castellano and F. Diederich, *Angew. Chem.*, 2003, **42**, 1210–1250.
- 22 J.-D. Chai and M. Head-Gordon, *Phys. Chem. Chem. Phys.*, 2008, **10**, 6615–6620.
- 23 T. H. Dunning Jr, *J. Chem. Phys.*, 1989, **90**, 1007–1023.
- 24 G. Cárdenas, J. Lucia-Tamudo, H. Mateo-de-laFuente, V. F. Palmisano, N. Anguita-Ortiz, L. Ruano, Á. Pérez-Barcia, S. Díaz-Tendero, M. Mandado and J. J. Nogueira, *ChemRxiv*, 2022, preprint, DOI: [10.26434/chemrxiv-2022-cnep2](https://doi.org/10.26434/chemrxiv-2022-cnep2).
- 25 F. Plasser, *J. Chem. Phys.*, 2020, **152**, 084108.
- 26 A. Nenov, R. Borrego-Varillas, A. Oriana, L. Ganzer, F. Segatta, I. Conti, J. Segarra-Martí, J. Omachi, M. Dapor and S. Taioli, *J. Phys. Chem. Lett.*, 2018, **9**, 1534–1541.
- 27 A. A. Blevins and G. Blanchard, *J. Phys. Chem. B*, 2004, **108**, 4962–4968.
- 28 C. R. Crecca and A. E. Roitberg, *J. Phys. Chem. A*, 2006, **110**, 8188–8203.
- 29 A. E. Raeber and B. M. Wong, *J. Chem. Theory Comput.*, 2015, **11**, 2199–2209.
- 30 X. Wang, S. Gao, M. Zhao and N. Marom, *Phys. Rev. Res.*, 2022, **4**, 033147.
- 31 M. Brylinski, *Chem. Biol. Drug Des.*, 2018, **91**, 380–390.
- 32 A. L. Ringer, M. O. Sinnokrot, R. P. Lively and C. D. Sherrill, *Chem. – Eur. J.*, 2006, **12**, 3821–3828.
- 33 M. O. Sinnokrot and C. D. Sherrill, *J. Phys. Chem. A*, 2006, **110**, 10656–10668.

